Theoretical Study of the Hydrogen and Chlorine Abstraction from Chloromethanes by Silyl and Trichlorosilyl Radicals: A Comparison between the Hartree−Fock Method, Perturbation Theory, and Density Functional Theory

Andrea Bottoni

Dipartimento di Chimica "G. Ciamician", Universita' di Bologna, via Selmi 2, 40126 Bologna, Italy

Received: May 7, 1998; In Final Form: September 16, 1998

We have carried out a theoretical study on the hydrogen and chlorine abstraction reactions by silyl ($H_3Si\cdot$) and trichlorosilyl ($Cl_3Si\cdot$) radical from the three chloromethanes $ClCH_3$, Cl_2CH_2, and Cl_3CH. The results of traditional ab initio methods (HF, MP2, and MP4) have been compared with those obtained with a DFT approach using the hybrid B3LYP and the pure BLYP functional. At all computational levels, we have found that the chlorine abstraction is highly favored with respect to the hydrogen abstraction as experimentally found. Furthermore, not only the Hartree−Fock method, as one can expect, but also correlated methods such as MP2 and MP4 largely overestimate the activation barriers. Only the DFT approach is able to provide results in good agreement with the experiment; in particular, the best performance has been obtained with the hybrid functional B3LYP which seems to be particularly suitable for investigating the reactivity of these types of radicals. A simple diabatic model based upon valence bond theory has been used to rationalize the reactivity pattern shown by these radical reactions.

Introduction

Alkyl radicals are known to react with haloalcanes mainly via hydrogen abstraction and not halogen abstraction. In contrast, many heteroatom-centered radicals are capable of abstracting a halogen atom from organic halides (see eq 1), and dehalogenation represents an important process that is frequently used in synthetic organic chemistry or to generate specific carbon-centered radicals for EPR spectroscopy or other purposes.

$$R'_nM\cdot + X{-}R = R'_nM{-}X + R\cdot$$

$$M = B, Si, Ge, P, \text{transition metal}; X = F, Cl, Br, I \quad (1)$$

Heteroatoms, which have been recognized to be involved in this type of process, are, for instance, boron[1], silicon,[2,3] germanium,[2,4] tin[2,5] phosphorus,[2,6] and various transition metals.[2b,7] In particular, the halogen abstraction carried out by silyl radicals has been widely investigated, and a large amount of experimental data concerning the reactivity of silicon-centered radicals toward different types of organic halides is now available[3]. For instance, the relative rates of chlorine atom abstraction from alkyl chlorides by the trimethylsilyl radical was studied in the gas phase by Cadman et al.[3c] These data, put on an absolute basis, provided a barrier of 4.06 kcal mol^{-1} for the chlorine abstraction from H_3CCl. Aloni et al.[3d] obtained the relative Arrhenius parameters for chlorine atom abstraction by trichlorosilyl radicals from chloromethane in the liquid phase. They found that the activation barrier decreases with the increasing number of halogen atoms and that their data, when compared with previously obtained results, were consistent with the assumption that the solvent effect is negligible for these reactions. More recently, the absolute rate constants for the reaction of triethylsilyl radicals with a number of organic halides RX were measured in solution by Chatgilialoglu et al.[3e−i] using laser flash photolysis techniques. These authors noticed that the trends in reactivity were consistent with those found in previous studies. In particular, they pointed out that for a given R the rate constants decrease along the series X = I > Br > Cl > F and that for a given X the trend is R = allyl > benzyl > *tert*-alkyl > *sec*-alkyl > primary alkyl.

Despite the growing interest in the chemistry and reactivity of silyl radicals and their extensive use in organic synthesis, not many theoretical investigations on the mechanistic aspects of these species are nowadays available. In particular, as far as we know, detailed theoretical studies of the halogen abstraction by silyl radicals and substituted silyl radicals and a comparison with the hydrogen abstraction process are still lacking. In this paper, we present the results of a theoretical study on the hydrogen and chlorine abstraction by silyl $H_3Si\cdot$ and trichlorosilyl $Cl_3Si\cdot$ radical from the three chloromethanes $ClCH_3$, Cl_2CH_2, and Cl_3CH. These radical reactions are particularly suitable for a theoretical investigation, since it has been experimentally demonstrated that the solvent effect is negligible.[3d] To investigate these reactions, we use the unrestricted Hartree−Fock (HF) method, the Moller−Plesset perturbation theory up to second and fourth order (MP2 and MP4), and the density functional theory (DFT) method with two different functionals. The paper has two aims. The first is to shed light on the mechanistic details (energetic and kinetics) of these important reactions to assess the relative importance of hydrogen and chlorine abstractions and the effect due to a change of the halogen involved in the process (comparison along the series F, Cl, Br). The second is to compare the accuracy of DFT techniques[8,9] with post-HF methods (like MP2 and MP4) in describing this class of reactions. This aspect is particularly relevant since during the past decade DFT has experienced a rise in its popularity for computing molecular properties and reactivity. This popularity is mainly due to the discovery of new and more accurate approximations to the exchange−correlation term in the energy functional[9] and to the computa-

10.1021/jp982166g CCC: $15.00
Published on Web 11/13/1998

tional expedience of DFT-based methods, which makes possible the inclusion of electron correlation in the computations of large molecular systems. Since during the last years only a few papers have appeared reporting a systematic comparison between traditional correlated ab initio methods and DFT-based methods,[10] a calibration of these methods for identifying strengths and weaknesses of each functional has become nowadays particularly important.

Computational Procedure. All the ab initio and DFT molecular computations reported here were performed with the Gaussian 94[11] series of programs using the 6-31G*[12a] and the 6-311G**[12b,c] basis sets. At the HF, MP2, and DFT levels, the geometrical parameters of the various critical points were fully optimized with the gradient method available in Gaussian 94. The nature of each critical point was characterized by computing the harmonic vibrational frequencies. As suggested by Sosa and Schlegel,[13] we used spin-projected MP2 and MP4 energies to cancel the spin contamination that affects the transition structures and which can cause an overestimation of the energy barriers.

For the DFT computations, we used a pure and a hybrid functional as implemented in Gaussian 94. The hybrid functional corresponds to the Becke's three-parameter exchange functional[9g] and is denoted here as B3LYP. When the Gaussian 94 formalism is followed, this functional can be written in the form

$$0.80E(\mathrm{S})_x + 0.20E(\mathrm{HF})_x + 0.72E(\mathrm{B88})_x + 0.19E(\mathrm{Local})_c + 0.81E(\mathrm{LYP})_c \quad (2)$$

where $E(\mathrm{S})_x$ is the Slater exchange,[9a,b] $E(\mathrm{HF})_x$ the Hartree−Fock exchange, $E(\mathrm{B88})_x$ represents the Becke's 1988 nonlocal exchange functional corrections,[9d] $E(\mathrm{Local})_c$ corresponds to the Vosko, Wilk, and Nusair (VWN) local correlation functional,[9c] and $E(\mathrm{LYP})_c$ corresponds to the correlation functional of Lee, Yang, and Parr,[9e,f] which includes both local and nonlocal terms. The pure DFT functional, denoted as BLYP, has the following expression:

$$E(\mathrm{S})_x + E(\mathrm{B88})_x + E(\mathrm{LYP})_c \quad (3)$$

Results and Discussion

A. Structures and Energetics. A schematic representation of the transition structures corresponding to the hydrogen (TS_1) and chlorine (TS_2) abstraction from $ClCH_3$, Cl_2CH_2, and Cl_3CH by silyl and trichlorosilyl radical is given in Figure 1. The most relevant geometrical parameters are reported in Tables 1 and 2. The bond lengths and bond angles given in these tables are defined in Figure 1. The energies relative to reactants of the two transition states, TS_1 and TS_2, are collected in Tables 3 and 4 for the silyl and trichlorosilyl radical, respectively. In addition to the energy values, we report also the zero-point vibrational energy corrections (ZPE, unscaled), the thermal corrections to enthalpy (H_{th}) at the temperature $T = 298$ K, and the corresponding activation energies (E_a). H_{th} is given by the expression

$$H_{th} = \mathrm{ZPE} + E_{vib} + E_{rot} + E_{tr} + RT$$

where E_{vib}, E_{rot}, and E_{tr} are the vibrational, rotational, and translational contributions to the energy, respectively, T is the absolute temperature, and R is the gas constant. The activation energy is obtained from the expression $E_a = \Delta H^{\ddagger} + nRT$, where $\Delta H^{\ddagger}$ is the activation enthalpy and n represents the molecularity of the reaction (2 for the reactions investigated here). The molecular enthalpy is computed as $H = E + H_{th}$, where E is the quantomechanical energy.

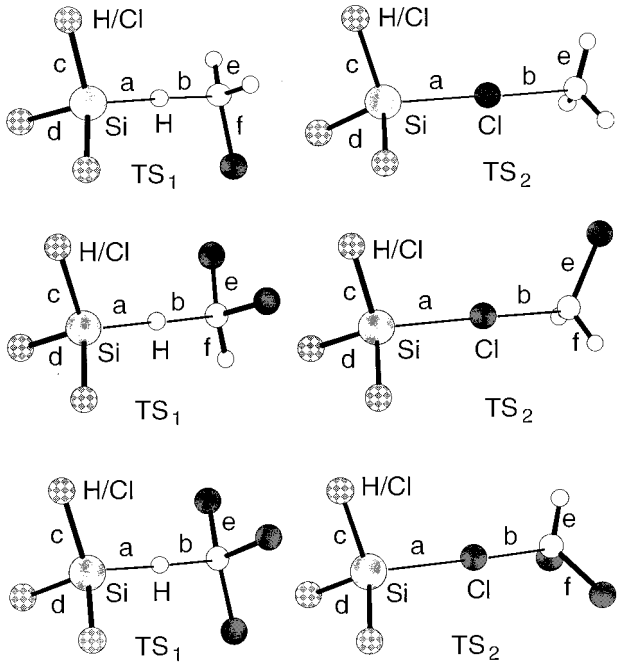

Figure 1. Schematic representation of the transition states for hydrogen (TS_1) and chlorine (TS_2) abstraction by silyl ($H_3Si\cdot$) and trichlorosilyl ($Cl_3Si\cdot$) radicals from chloromethanes.

In all cases, we have found that both hydrogen and chlorine abstractions proceed in one step and that the three atoms involved in the process are in a collinear or almost collinear arrangement. Furthermore, while in the hydrogen abstraction transition state, both the $H_3Si\cdot$ and $Cl_3Si\cdot$ radicals approach the hydrogen atom of the substrate in a staggered conformation; in the chlorine abstraction transition state, they are in an eclipsed conformation. For all transition structures, the frequency analysis has shown that the transition vector associated with the imaginary frequency is a linear combination of the breaking and forming bonds (parameters a and b in Figure 1).

To check the reliability of our computational approach, we first discuss in detail the reactions involving the silyl radical $H_3Si\cdot$. Before discussing the structural features of the two transition states TS_1 and TS_2, we introduce the quantity θ (reported in Tables 1 and 2), which conveniently describes the change of character of the various transition structures determined at different computational levels. For the H abstraction, θ is defined as $\theta = \delta R(\mathrm{Si-H})/\delta R(\mathrm{C-H})$, where $\delta R(\mathrm{Si-H}) = a/R(\mathrm{Si-H})_{eq}$ and $\delta R(\mathrm{C-H}) = b/R(\mathrm{C-H})_{eq}$. Here, a and b are the lengths of the forming Si−H and breaking C−H bonds, respectively, as reported in Table 1 and $R(\mathrm{Si-H})_{eq}$ and $R(\mathrm{C-H})_{eq}$ are the corresponding equilibrium distances in the product (silane) and reactant (chloromethane). In a similar way for the Cl abstraction, θ is defined as $\theta = \delta R(\mathrm{Si-Cl})/\delta R(\mathrm{C-Cl})$, where $\delta R(\mathrm{Si-Cl}) = a/R(\mathrm{Si-Cl})_{eq}$ and $\delta R(\mathrm{C-Cl}) = b/R(\mathrm{C-Cl})_{eq}$. In this case, a and b are the lengths of the forming Si−Cl and breaking C−Cl bonds, respectively, and $R(\mathrm{Si-Cl})_{eq}$ and $R(\mathrm{C-Cl})_{eq}$ are the corresponding equilibrium distances in the product (chlorosilane) and reactant (chloromethane). A value of 1 for θ indicates a transition state where the two bonds are broken and formed to the same extent; a value lower or higher than 1 corresponds to a more product-like or to a more reactant-like transition state, respectively. In the present case, inspection of the results reported in Table 1 points out the product-like character of TS_1 ($\theta < 1$) and the reactant-like character of TS_2

TABLE 1: Optimum Values[a] of the Most Relevant Geometrical Parameters of the Transition States for Hydrogen Abstraction (TS_1) and Chlorine Abstraction (TS_2) by Silyl Radical from $ClCH_3$, Cl_2CH_2, and Cl_3CH Obtained with the 6-31G* and the 6-311G (Values in Parenthesis) Basis Sets at Various Levels of Theory**

	HF	MP2	B3LYP	BLYP
		(a) $H_3Si\cdot + ClCH_3$		
		TS_1		
a	1.711	1.644 (1.626)	1.642 (1.639)	1.639 (1.637)
b	1.445	1.512 (1.509)	1.552 (1.549)	1.600 (1.595)
∠ab	177.7	176.5 (177.9)	179.6 (179.7)	179.5 (179.3)
∠ac	108.8	109.3 (108.7)	109.3 (108.9)	109.5 (109.1)
∠be	104.9	103.3 (103.2)	102.5 (102.6)	102.0 (102.2)
∠bf	107.6	107.6 (107.2)	108.8 (108.7)	109.7 (109.6)
θ	0.865	0.798	0.776	0.752
		TS_2		
a	2.568	2.435 (2.441)	2.541 (2.567)	2.606 (2.635)
b	2.056	2.001 (2.000)	2.010 (2.027)	2.082 (2.039)
∠ab	180.0	180.0 (180.0)	180.0 (180.0)	180.0 (180.0)
∠ac	108.5	108.3 (107.8)	108.4 (107.7)	108.4 (107.6)
∠be	103.9	105.0 (105.0)	104.8 (104.2)	104.9 (104.2)
θ	1.078	1.051	1.097	1.091
		(b) $H_3Si\cdot + Cl_2CH_2$		
		TS_1		
a	1.715	1.648 (1.631)	1.661 (1.656)	1.663 (1.660)
b	1.431	1.493 (1.488)	1.506 (1.508)	1.539 (1.538)
∠ab	177.5	176.4 (178.5)	179.1 (179.8)	179.8 (179.0)
∠ac	108.8	108.5 (108.9)	108.9 (108.9)	109.0 (109.0)
∠be	106.7	106.3 (106.1)	106.9 (106.9)	107.5 (107.5)
∠bf	105.1	103.9 (104.0)	103.4 (104.0)	103.2 (103.7)
θ	0.872	0.809	0.807	0.791
		TS_2		
a	2.609	2.472 (2.476)	2.633 (2.653)	2.740 (2.759)
b	2.020	1.975 (1.976)	1.975 (1.988)	1.971 (1.992)
∠ab	179.6	178.9 (178.3)	177.8 (178.8)	176.1 (177.3)
∠ac	107.9	107.7 (107.5)	107.9 (106.9)	107.8 (106.9)
∠be	111.5	111.9 (112.0)	112.6 (112.5)	113.2 (113.1)
∠bf	103.5	104.3 (104.2)	104.2 (103.9)	104.6 (104.0)
θ	1.105	1.075	1.149	1.203
		(c) $H_3Si\cdot + Cl_3CH$		
		TS_1		
a	1.717	1.646	1.671	1.676
b	1.416	1.480	1.476	1.500
∠ab	180.0	180.0	180.0	180.0
∠ac	108.1	108.4	108.5	108.6
∠be	105.5	105.1	105.5	105.9
θ	0.881	0.814	0.827	0.816
		TS_2		
a	2.654	2.514	2.741	2.909
b	1.991	1.950	1.935	1.925
∠ab	179.7	179.0	177.9	176.4
∠ac	107.5	107.2	107.1	106.9
∠be	102.7	103.9	104.2	104.9
∠bf	109.6	109.8	110.4	110.8
θ	1.137	1.105	1.218	1.305

[a] Bond lengths are in angstroms, and angles are in degrees.

TABLE 2: Optimum Values[a] of the Most Relevant Geometrical Parameters of the Transition States for Hydrogen Abstraction (TS_1) and Chlorine Abstraction (TS_2) by Trichlorosilyl Radical from $ClCH_3$, Cl_2CH_2, and Cl_3CH Obtained with the 6-31G* Basis Set at Various Levels of Theory

	HF	MP2	B3LYP	BLYP
		(a) $Cl_3Si\cdot + ClCH_3$		
		TS_1		
a	1.699	1.633	1.615	1.598
b	1.420	1.491	1.569	1.664
∠ab	179.6	176.6	178.6	178.0
∠ac	108.4	109.4	108.9	108.9
∠be	104.3	102.9	101.4	100.2
∠bf	107.2	106.8	108.2	108.7
θ	0.887	0.811	0.763	0.712
		TS_2		
a	2.475	2.376	2.438	2.476
b	2.063	1.993	2.027	2.047
∠ab	180.0	180.0	180.0	180.0
∠ac	110.1	110.1	110.1	110.0
∠be	103.3	104.6	103.9	103.8
∠bf	2.063	1.993	2.027	2.047
θ	1.055	1.046	1.060	1.068
		(b) $Cl_3Si\cdot + Cl_2CH_2$		
		TS_1		
a	1.709	1.642	1.642	1.629
b	1.402	1.464	1.510	1.581
∠ab	179.3	176.1	179.4	178.6
∠ac	110.8	109.7	110.7	110.5
∠be	106.3	105.6	106.3	106.7
∠bf	104.6	103.7	102.4	101.6
θ	0.901	0.830	0.804	0.762
		TS_2		
a	2.522	2.419	2.536	2.616
b	2.034	1.969	1.989	1.995
∠ab	179.2	178.2	176.1	173.6
∠ac	110.1	110.1	110.8	111.0
∠be	111.1	111.6	112.2	112.6
∠bf	102.6	103.8	103.3	103.5
θ	1.080	1.072	1.116	1.150
		(c) $Cl_3Si\cdot + Cl_3CH$		
		TS_1		
a	1.716	1.644	1.658	1.647
b	1.387	1.445	1.471	1.530
∠ab	179.9	180.0	179.5	179.5
∠ac	109.2	109.3	109.4	109.6
∠be	105.1	104.6	104.9	104.9
θ	0.912	0.841	0.832	0.794
		TS_2		
a	2.571	2.463	2.636	2.767
b	2.010	1.947	1.955	1.950
∠ab	179.4	178.7	176.9	174.3
∠ac	109.1	109.0	108.6	108.1
∠be	101.5	103.2	103.0	103.6
∠bf	109.1	109.4	109.8	110.2
θ	1.111	1.102	1.177	1.242

[a] Bond lengths are in angstroms, and angles are in degrees.

($\theta > 1$). Furthermore, the change of θ indicates that TS_1 becomes less product-like while TS_2 becomes more reactant-like when more chlorine atoms are introduced in the substrate (at the HF level for TS_1, θ changes from 0.865 to 0.872 and 0.881 on passing from $ClCH_3$ to Cl_2CH_2 and Cl_3CH; the corresponding θ values found for TS_2 are 1.078, 1.105, and 1.137). The inclusion of the dynamic correlation energy at the MP2 level has the effect of making the forming bonds shorter and the breaking bonds longer in both TS_1 and TS_2. As a consequence, TS_1 becomes more product-like (θ is smaller than 1 and further decreases) and TS_2 less reactant-like (θ is larger than 1 and decreases). A similar effect has been found for TS_1 at the DFT (B3LYP and BLYP) level; with both functionals, θ further decreases with respect to the HF value. An opposite effect is observed for TS_2, where θ significantly increases with respect to the HF value.

Even if the activation barriers for the chlorine abstraction by silyl radicals from chlorometanes are not experimentally available, to roughly estimate the reliability of our computed activation energies E_a we can compare them with the experimental values determined for chlorine abstraction by triethylsilyl radicals $Et_3Si\cdot$ from $ClCH_3$, Cl_2CH_2 and Cl_3CH; these barriers are 4.06, 2.06, and 1.14 kcal mol^{-1}, respectively.[1f] Inspection

TABLE 3: Energies (E, kcal mol^{-1}) Relative to Reactants,[a] Activation Energies (E_a, kcal mol^{-1}), Zero-Point Energy Corrections (ZPE, kcal mol^{-1}), and Thermal Corrections (H_{th}, kcal mol^{-1}) Computed for Hydrogen (TS_1) and Chlorine Abstraction (TS_2) by Silyl Radical from $ClCH_3$, Cl_2CH_2, and Cl_3CH with the 6-31G* and 6-311G (Values in Parenthesis) Basis Sets at Various Levels of Theory**

	HF	MP2	MP4	B3LYP	BLYP
		(a) $H_3Si^{\bullet} + ClCH_3$			
		reactants			
ZPE	39.89	38.48		37.29	36.21
H_{th}	44.79	43.39		42.25	41.20
		TS_1			
E	30.89	26.19 (22.87)	(23.48)	19.72 (19.56)	17.89 (17.95)
ZPE	38.82	35.44		34.38	33.37
H_{th}	41.22	39.90		38.88	37.92
E_a	28.33	23.78 (20.46)	(21.07)	17.43 (17.27)	15.69 (15.75)
		TS_2			
E	21.54	14.24 (13.70)	(14.02)	7.42 (7.75)	4.62 (4.95)
ZPE	39.52	38.39		37.18	36.09
H_{th}	44.27	43.11		42.07	41.0
E_a	22.10	15.04(14.50)	(14.82)	8.32 (8.65)	5.58 (5.91)
		(b) $H_3Si^{\bullet} + Cl_2CH_2$			
		reactants			
ZPE	34.46	33.12 (00.00)		31.98	30.92
H_{th}	39.67	38.36		37.28	36.28
		TS_1			
E	28.74	22.14 (18.77)	(17.62)	16.11 (16.11)	13.96 (14.21)
ZPE	31.29	30.05		29.03	28.06
H_{th}	36.22	35.04		34.10	33.20
E_a	26.37	19.90 (16.53)	(15.38)	14.01 (14.01)	11.96 (12.21)
		TS_2			
E	19.36	13.88 (11.10)	(11.14)	5.17 (5.54)	2.52 (2.84)
ZPE	34.36	33.29		32.08	31.04
H_{th}	39.51	38.41		37.41	36.48
E_a	20.28	15.01 (12.23)	(12.27)	6.38 (6.75)	3.80 (4.12)
		(c) $H_3Si^{\bullet} + Cl_3CH$			
		reactants			
ZPE	28.17	27.01		25.91	24.94
H_{th}	33.87	32.77		31.78	30.90
		TS_1			
E	26.27	18.32		12.95	10.67
ZPE	25.05	24.02		23.02	22.11
H_{th}	30.60	29.67		28.79	27.99
E_a	24.08	16.30		11.04	8.84
		TS_2			
E	16.55	8.46		2.89	0.65
ZPE	28.31	27.39		26.15	25.16
H_{th}	34.04	33.11		31.54	30.72
E_a	17.80	9.88		3.73	1.55

[a] The absolute energies (hartrees) of the reactants are as follows. (a) $H_3Si^{\bullet} + ClCH_3$: −789.699 27 (HF), −790.029 58 (−790.154 83) (MP2), (−790.216 42) (MP4), −791.340 80 (−791.411 79) (B3LYP), −791.254 10 (−791.331 08) (BLYP). (b) $H_3Si^{\bullet} + Cl_2CH_2$: −1248.591 30 (HF), −1249.051 02 (−1249.202 34) (MP2), (−1249.274 35) (MP4), −1250.928 64 (−1251.026 75) (B3LYP), −1250.831 66 (−1250.937 69) (BLYP). (c) $H_3Si^{\bullet} + Cl_3CH$: −1707.475 83 (HF), −1708.069 38 (MP2), −1710.511 39 (B3LYP), −1710.404 77 (BLYP).

TABLE 4: Energies Relative to Reactants (E, kcal mol^{-1}), Activation Energies (E_a, kcal mol^{-1}), Zero-Point Energy Corrections (ZPE, kcal mol^{-1}), and Thermal Corrections (H_{th}, kcal mol^{-1}) Computed for Hydrogen (TS_1) and Chlorine Abstraction (TS_2) by Trichlorosilyl Radical from $ClCH_3$, Cl_2CH_2, and Cl_3CH with the 6-31G* Basis Set at Various Levels of Theory

	HF	MP2	B3LYP	BLYP
		(a) $Cl_3Si^{\bullet} + ClCH_3$		
		reactants		
ZPE	28.93		26.98	26.12
H_{th}	35.11		33.32	32.54
		TS_1		
E	29.19	22.91	19.58	18.85
ZPE	25.09		23.28	22.62
H_{th}	31.32		29.65	29.05
E_a	26.48	20.20	16.99	16.44
		TS_2		
E	20.54	10.54	6.74	4.30
ZPE	27.72		26.08	25.25
H_{th}	34.27		32.83	32.14
E_a	20.78	10.78	7.33	4.98
		(b) $Cl_3Si^{\bullet} + Cl_2CH_2$		
		reactants		
ZPE	23.50		21.66	20.85
H_{th}	29.98		28.35	27.62
		TS_1		
E	28.44	19.39	16.76	15.49
ZPE	19.45		17.85	17.16
H_{th}	26.25		24.87	24.27
E_a	25.79	16.74	14.36	13.22
		TS_2		
E	19.55	8.75	5.22	2.70
ZPE	22.54		21.06	20.32
H_{th}	29.51		28.23	27.64
E_a	20.16	9.36	6.18	3.80
		(c) $Cl_3Si^{\bullet} + Cl_3CH$		
		reactants		
ZPE	17.21		15.59	14.86
H_{th}	24.19		22.85	22.24
		TS_1		
E	27.05	15.91	14.32	12.86
ZPE	13.10		11.79	11.16
H_{th}	20.59		19.55	19.06
E_a	24.97	13.83	12.10	10.76
		TS_2		
E	17.61	6.44	3.58	1.36
ZPE	16.50		15.20	14.56
H_{th}	24.05		23.00	22.52
E_a	18.55	7.38	4.81	2.72

[a] The absolute energies (hartrees) of reactants are as follows. (a) $Cl_3Si^{\bullet} + ClCH_3$: −2166.567 69 (HF), −2167.278 30 (MP2), −2170.289 30 (B3LYP), −2170.167 30 (BLYP). (b) $Cl_3Si^{\bullet} + Cl_2CH_2$: −2625.459 74 (HF), −2626.299 74 (MP2), −2629.877 14 (B3LYP), −2629.744 89 (BLYP). (c) $Cl_3Si^{\bullet} + Cl_3CH$: −3084.344 27 (HF), −3085.318 10 (MP2), −3089.459 86 (B3LYP), −3089.317 97 (BLYP).

of Table 3 shows that the corresponding values determined at the HF level are much larger, i.e., 22.10, 20.28, and 17.80 kcal mol^{-1} for $ClCH_3$, Cl_2CH_2, and Cl_3CH, respectively. These barriers are in all cases smaller than the corresponding values associated with the H abstraction, in agreement with the experimental observation that substituted silyl radicals ($R_3Si^{\bullet}$ or $Cl_3Si^{\bullet}$) react with haloalkanes via halogen abstraction and not hydrogen abstraction. Also, the decrease of E_a along the series is in agreement with the experiment. The large overestimate of the barriers provided by the HF model is not surprising since it is well-known that the accurate predictions of the energy barriers of radical reactions is a difficult problem and high levels of theory including dynamic correlation are usually needed for reproducing the experimental values.[13] A significant decrease of the activation energies is observed when the projected MP2 approach is used, even if the results obtained at this level of theory are still quite overestimated; the computed values are 15.04, 15.01, and 9.88 kcal mol^{-1} for chloro-, dichloro-, and trichloromethane, respectively.

The DFT approach provides much better results. The two sets of energy barriers obtained with the B3LYP and BLYP functionals are both quite close to the experimental values

determined for $Et_3Si^{\bullet}$; in the first case (B3LYP), we obtain 8.32, 6.38, and 3.73 kcal mol^{-1}, while at the BLYP level these values become 5.58, 3.80, and 1.55 kcal mol^{-1}, respectively. Furthermore, as also found at the HF and MP2 levels, at the DFT level the barrier for hydrogen abstraction is much higher than the corresponding barrier for chlorine abstraction, which indicates that in all cases this process is highly favored. However, it is difficult in the present case to assess what functional provides the best agreement with the experiment, since in our computations we neglect the effect of the ethyl groups bonded to silicon.

To obtain a better reference and to test the reliability of the 6-31G* basis, we have carried out MP2, MP4, B3LYP, and BLYP computations with the 6-311G** basis set on the reactions involving $ClCH_3$ and Cl_2CH_2. In these computations, we have again optimized the geometrical parameters of reactant and transition states at the MP2, B3LYP, and BLYP levels using the more accurate basis set and we have carried out single-point MP4 computations on the MP2 optimized geometries. Also, at the MP4 level we have taken the spin-projected energy values. To evaluate the activation energies E_a, we have used the thermal corrections obtained with the 6-31G* basis. These results are reported in Tables 1 and 3 in parentheses. It is interesting to note that a triple-ζ basis including p polarization functions on the hydrogen atoms does not change significantly either the optimum geometrical parameters or the E_a values. At the MP2, B3LYP, and BLYP levels, the barriers for Cl abstraction become 14.50, 8.65, and 5.58 kcal mol^{-1} for $ClCH_3$ and 12.23, 6.75 and 4.12 kcal mol^{-1} for Cl_2CH_2. Also, the inclusion of perturbation corrections up to fourth order (MP4) leaves almost unchanged the energetics of the reactions with respect to the MP2 level.

In summary, the results obtained for the reaction between $H_3Si^{\bullet}$ and chloromethanes indicate that the DFT approach can provide much better results than traditional correlated methods such as MP2 and MP4 and that the 6-31G* basis set can be adequate for describing these systems.

We discuss now the results obtained for the reaction between $Cl_3Si^{\bullet}$ and chlorometanes. In this case, we have used only the 6-31G* basis at the HF, MP2, and DFT levels of theory. The structural features of the two transition states TS_1 and TS_2 found for $Cl_3Si^{\bullet}$ (see Table 2) are very similar to those of the corresponding structures already discussed for $H_3Si^{\bullet}$. As found before, TS_1 has a product-like character ($\theta < 1$) while TS_2 has a reactant-like character ($\theta > 1$). TS_1 becomes again less product-like, while TS_2 becomes more reactant-like along the series $ClCH_3$, Cl_2CH_2, and Cl_3CH. Also, the effect of the dynamic correlation is similar to that previously pointed out for $H_3Si^{\bullet}$; the product-like character of TS_1 increases at the MP2 and DFT levels, while the reactant-like character of TS_2 decreases at the MP2 level and then increases again at the DFT level.

For the chlorine abstraction reaction by $Cl_3Si^{\bullet}$ from chloromethanes, the Arrhenius parameters experimentally available are relative to the bromine atom abstraction from cyclohexyl bromide. We can roughly put these data on a absolute basis by assuming the activation energy for bromine abstraction to be about 1 kcal mol^{-1}. This assumption can be justified on the basis of the experimental values of the activation energies for bromine abstraction by triethylsilyl radicals from different substrates. This barrier is 1.3 ± 0.5 kcal mol^{-1} for $C_6H_5CH_2Br$, 0.85 ± 0.13 kcal mol^{-1} for $(CH_3)_3CBr$, and 0.72 ± 0.35 kcal mol^{-1} for $CH_3(CH_2)_4Br$.[3e] Under this assumption, we obtain a set of experimental activation energies for chlorine abstraction by $Cl_3Si^{\bullet}$ from chloromethanes that we can compare to our computed activation energies. These experimental values are 6.18, 5.60, and 4.40 kcal mol^{-1} for $ClCH_3$, Cl_2CH_2, and Cl_3CH, respectively.

TABLE 5: Values of $\langle S^2 \rangle$ Computed at the HF, MP2, B3LYP, and BLYP Levels with the 6-31G* Basis Set for the Hydrogen Abstraction (TS_1) and Chlorine Abstraction (TS_2) Transition States for the Reactions between Silyl or Trichlorosilyl Radical and $ClCH_3$, Cl_2CH_2, and Cl_3CH

	HF	MP2	B3LYP	BLYP
Hydrogen Abstraction (TS_1)				
$H_3Si^{\bullet} + ClCH_3$	0.7885	0.7624	0.7562	0.7535
$H_3Si^{\bullet} + Cl_2CH_2$	0.7872	0.7622	0.7559	0.7532
$H_3Si^{\bullet} + Cl_3CH$	0.7852	0.7821	0.7554	0.7529
$Cl_3Si^{\bullet} + ClCH_3$	0.7883	0.7624	0.7561	0.7533
$Cl_3Si^{\bullet} + Cl_2CH_2$	0.7880	0.7626	0.7558	0.7530
$Cl_3Si^{\bullet} + Cl_3CH$	0.7869	0.7623	0.7555	0.7527
Chlorine Abstraction (TS_2)				
$H_3Si^{\bullet} + ClCH_3$	0.8543	0.7900	0.7606	0.7549
$H_3Si^{\bullet} + Cl_2CH_2$	0.8504	0.7895	0.7592	0.7538
$H_3Si^{\bullet} + Cl_3CH$	0.8442	0.7885	0.7572	0.7529
$Cl_3Si^{\bullet} + ClCH_3$	0.8507	0.7861	0.7605	0.7547
$Cl_3Si^{\bullet} + Cl_2CH_2$	0.8525	0.7880	0.7558	0.7530
$Cl_3Si^{\bullet} + Cl_3CH$	0.8523	0.7883	0.7576	0.7529

Inspection of Table 4 shows that at all computational levels of theory the trend of the energy barriers is the same as that found for $H_3Si^{\bullet}$ (the process of chlorine abstraction is favored with respect to hydrogen abstraction, and the barriers decrease with the increasing number of chlorine atoms in the substrate). As found for $H_3Si^{\bullet}$, the barriers are largely overestimated not only at the HF level (where the error is higher than 200%) but also at the MP2 level. At the DFT level, both functionals provide much better results. The computed activation energies for chlorine abstraction from $ClCH_3$, Cl_2CH_2, and Cl_3CH are 7.33, 6.18, and 4.81 kcal mol^{-1} at the B3LYP level and 4.98, 3.80, and 2.72 kcal mol^{-1} at the BLYP level. These values must be compared with 6.18, 5.60, and 4.40 kcal mol^{-1}, respectively. Thus, the best agreement with the experiment is found at the B3LYP level where the error ranges between 9% and 18%.

The results obtained for $Cl_3Si^{\bullet}$ are a further indication of the reliability of the DFT approach in dealing with this type of radicals. In particular, they suggest that the hybrid B3LYP functional and not the pure BLYP functional can provide the best agreement with the experiment. Another aspect that is worth discussing briefly is the ability of the DFT-based methods to reduce the effect of the spin contamination on the wave function. This decrease of spin contamination, which should provide more reliable geometrical parameters, is evident from the values of $\langle S^2 \rangle$ (see Table 5) computed at the HF, MP2, B3LYP, and BLYP levels for the two transition states TS_1 and TS_2 for the reactions between $H_3Si^{\bullet}$ or $Cl_3Si^{\bullet}$ and chloromethanes.

It is also interesting to point out that the two sets of data obtained for $H_3Si^{\bullet}$ and $Cl_3Si^{\bullet}$ are characterized by the same trends and that the effect due to the substitution of the three hydrogen atoms with three chlorine atoms on the energy barriers is not very large. This finding suggests that we can use the silyl radical $H_3Si^{\bullet}$ as a reliable model system to investigate a number of reactions involving substituted silyl radicals. We follow this approach in the following section, where we try to understand the key factors that determine the general features of these radical abstractions by means of a simple diabatic model applied to $H_3Si^{\bullet}$.

B. Diabatic Model. The diabatic model used here is based upon spin recoupling in VB theory.[10e,14] Within this model, at any point along the reaction coordinate the total wave function

is represented (see eq 4) by a linear combination of two configurations Φ_R and Φ_P, which describe the electron coupling of reactants and products, respectively.

$$\Psi = a\Phi_R + b\Phi_P \quad (4)$$

At the beginning of the reaction, Φ_R is much lower in energy than Φ_P and is the dominant contribution ($a \gg b$). When we move from reactants to products, the importance of Φ_R decreases (its energy increases) and that of Φ_P increases (its energy decreases). In the transition-state region, the two configurations become almost degenerate and the two corresponding contributions are approximately equivalent. After the transition state, on the product side along the reaction coordinate, Φ_P becomes lower in energy than Φ_R and consequently dominates ($b \gg a$). Within this scheme, the variation of the relative importance of Φ_R and Φ_P describes the change from the reactant electron coupling to the product electron coupling corresponding to the process of breaking covalent bonds and forming new bonds, which occurs in most organic reactions.

This process can be conveniently represented in a diagram where we report the energy of the reacting system versus the reaction coordinate and where the total energy profile is decomposed into two component curves denoted as *reactant diabatic* and *product diabatic*, respectively. The former describes the energy behavior of the reactant configuration Φ_R (reactant spin coupling = reactant bonding situation), and the latter describes that of the product configuration Φ_P (product spin coupling = product bonding situation). The reactant diabatic, on passing from reactants to products, is repulsive, while the product diabatic is attractive. The crossing between the two diabatics determines the position of the transition state and the magnitude of the activation energy.

This scheme is applied here to the model system formed by the $H_3Si\cdot$ radical reacting with chloromethanes with the purpose of rationalizing the following points: (i) the larger barrier that characterizes the hydrogen abstraction with respect to the chlorine abstraction, (ii) the decrease for a given substrate of the rate constants for halogen abstraction along the series X = I > Br > Cl > F, (iii) the decrease of the chlorine abstraction barrier with the increasing number of the chlorine atoms in chloromethanes, and (iv) the different reactivities shown by silyl and alkyl radicals (the former reacts mainly via chlorine abstraction, while the latter reacts via hydrogen abstraction).

In Figure 2, we have represented the qualitative behavior of the reactant and product diabatics for the hydrogen abstraction and chlorine abstraction by the silyl radical $H_3Si\cdot$ from $ClCH_3$. For the hydrogen abstraction, the reactant diabatic corresponds to a situation where the pσ electron on the carbon atom of the halomethane molecule and the 1s electron on hydrogen are singlet spin coupled to form a C−H bond (reactant configuration Φ_R), while in the product diabatic, the singlet spin coupling occurs between the hydrogen 1s electron and the pσ electron on silicon to form the new Si−H bond (product configuration Φ_P). For the halogen abstraction in the reactant diabatic, the pσ electron on the carbon atom and the 3p electron on the chlorine atom are singlet spin coupled to form the C−Cl bond, while in the product diabatic, the 3p electron on chlorine is coupled to a singlet with the pσ electron on silicon to form the new Si−Cl bond in $ClSiH_3$. The reactant and product configurations are schematically represented in the two coupling schemes reported at the bottom of Figure 2.

In this type of diagrams, the position of the crossing and consequently the size of the barrier is determined by three factors: (i) the energy difference between the product diabatic

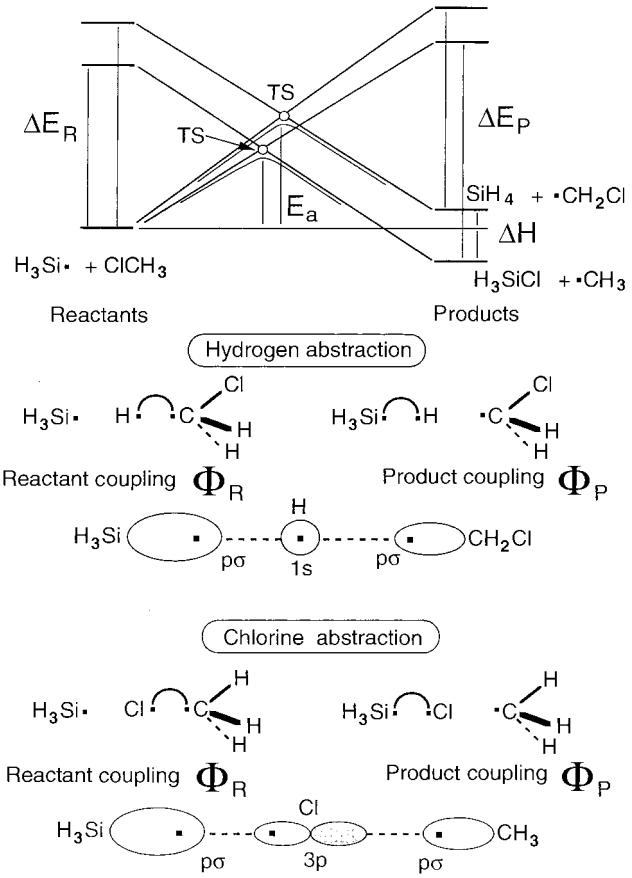

Figure 2. Correlation diagrams for hydrogen and chlorine abstraction by the $H_3Si\cdot$ radical from $ClCH_3$ and schematic representations of the reactant and product configurations.

at the product geometry and the reactant diabatic at the reactant geometry, which corresponds approximately to the reaction enthalpy (ΔH); (ii) the energy difference between the reactant and product diabatic at the reactant geometry (ΔE_R on the left side of the diagram); (iii) the energy difference between the reactant and product diabatic at the product geometry (ΔE_P on the right side of the diagram).

ΔH can be estimated on the basis of the computed quantomechanical energy values of the reactants and products. The energies of the products, relative to reactants, for the hydrogen abstraction and chlorine abstraction by $H_3Si\cdot$ from chloromethanes are reported in Table 6 together with the energy thermal corrections and the resulting values of reaction enthalpies ΔH (6-31G*/B3LYP computational level). These values show that while the hydrogen abstraction is endothermic, the chlorine abstraction is exothermic. Since in the diabatic diagram of Figure 2 we refer to the reaction between $H_3Si\cdot$ and $ClCH_3$, ΔH is 8.83 kcal mol^{-1} for the hydrogen abstraction and −16.22 kcal mol^{-1} for the chlorine abstraction.

The evaluation of ΔE_R and ΔE_P is less obvious. ΔE_R represents the energy required for decoupling the electron pair associated with the C−H bond in the case of hydrogen abstraction or the electron pair associated with the C−Cl bond in the case of chlorine abstraction. The variation of this quantity in the comparison between the two processes can be approximately evaluated from the energies of the C−H bond (about 100.9 kcal mol^{-1}[115]) or the C−Cl bond in $ClCH_3$ (about 83.5 kcal mol^{-1} [16]). In a similar way, we can evaluate the magnitude of ΔE_P, which represents the energy required for decoupling the electron pair of the Si−H bond in the case of hydrogen abstraction or the electron pair of the Si−Cl bond in

TABLE 6: Energies Relative[a] to Reactants (E, kcal mol^{-1}), Reaction Enthalpies (ΔH, kcal mol^{-1}), Zero-Point Energy Corrections (ZPE, kcal mol^{-1}), and Thermal Corrections (H_{th}, kcal mol^{-1}) Computed for the Products of the Hydrogen and Chlorine Abstraction by Silyl Radical from $ClCH_3$, Cl_2CH_2, and Cl_3CH at the B3LYP Level with the 6-31G* Basis Set

	E	ZPE	H_{th}	ΔH
	Hydrogen Abstraction			
$H_3Si\cdot + ClCH_3$	11.78	33.94	39.31	8.83
$H_3Si\cdot + Cl_2CH_2$	6.80	29.58	34.98	4.79
$H_3Si\cdot + Cl_3CH$	2.65	24.13	30.05	1.21
	Chlorine Abstraction			
$H_3Si\cdot + ClCH_3$	−17.91	35.29	40.57	−16.22
$H_3Si\cdot + Cl_2CH_2$	−25.57	30.84	36.43	−25.01
$H_3Si\cdot + Cl_3CH$	−33.74	26.48	32.10	−34.35

[a] The absolute energies (hartrees) of reactants are as follows. (i) $H_3Si\cdot + ClCH_3$: −791.340 80. (ii) $H_3Si\cdot + Cl_2CH_2$: −1250.928 64. (iii) $H_3Si\cdot + Cl_3CH$: −1710.511 39.

TABLE 7: Optimum Values[a] of the Most Relevant Geometrical Parameters of the Transition States for Fluorine and Bromine Abstraction by Silyl Radical from FCH_3 and $BrCH_3$ Obtained with the 6-31G* Basis Set at the B3LYP Level

	$H_3Si\cdot + FCH_3$	$H_3Si\cdot + BrCH_3$
a	2.016	2.843
b	1.658	2.088
∠ab	157.1	180.0
∠ac	100.4	107.9
∠be	103.8	105.6

[a] Bond lengths are in angstroms, and angles are in degrees.

the case of chlorine abstraction. Also, in this case we can approximately evaluate ΔE_P from the energies of the Si−H and Si−Cl bonds, which are 94.0[17] and 110.0 kcal mol^{-1},[18] respectively.

From the diagram of Figure 2, it is evident that while the effect of the change of ΔE_P in the comparison between hydrogen and chlorine abstraction is that of favoring the hydrogen abstraction, the effect of the variation of ΔH and ΔE_R is opposite. Since ΔH and ΔE_R dominate, the final overall effect of the simultaneous variation of ΔH, ΔE_R, and ΔE_P is a significantly larger energy barrier for the hydrogen abstraction than for the chlorine abstraction process as found in our computations and at the experimental level. It is worth pointing out that the diagram of Figure 2 also provides information on the nature of the two transition states; the relative positions of the two crossing points indicates that the transition state for hydrogen abstraction is more product-like than the transition state for chlorine abstraction. This is in agreement with the computed values of the θ parameter, which is always lower than 1 (product-like character) in the former case and greater than 1 (reactant-like character) in the latter.

Another aspect that can be easily rationalized by means of a diabatic model is the experimental observation that for a given substrate the rate constants for halogen abstraction decrease along the series X = I > Br > Cl > F (for iodides and for some bromides the halogen abstraction occurs at a rate that is equal or very close to the diffusion limit[3e]). In the following discussion, we compare bromine, chlorine, and fluorine. To evaluate the activation energies also for fluorine and bromine abstraction, we have computed at the B3LYP/6-31G* level the transition states for the reactions between $H_3Si\cdot$ and FCH_3 or $BrCH_3$. The most relevant geometrical parameters are reported in Table 7, and the corresponding energy values and activation energies are shown in Table 8. The computed E_a values for

TABLE 8: Energies Relative to Reactants[a] (E, kcal mol^{-1}), Activation Energies (E_a, kcal mol^{-1}), Zero-Point Energy Corrections (ZPE, kcal mol^{-1}), and Thermal Corrections (H_{th}, kcal mol^{-1}) Computed for Fluorine and Bromine Abstraction by Silyl Radical from FCH_3 and $BrCH_3$ with the 6-31G* Basis Set at the B3LYP Level

	$H_3Si\cdot + FCH_3$	$H_3Si\cdot + BrCH_3$
	Reactants	
ZPE	38.17	36.93
H_{th}	43.00	41.96
	Transition State	
E	17.45	−0.22
ZPE	37.47	37.03
H_{th}	42.24	42.10
E_a	17.71	1.00
	Products	
E	−33.05	−21.14
ZPE	36.09	35.15
H_{th}	41.23	40.48
ΔH	−34.88	−22.62

[a] The absolute energies (hartrees) of reactants at the B3LYP/6-31G* level are −430.966 17 (fluorine abstraction) and −2902.719 67 (bromine abstraction).

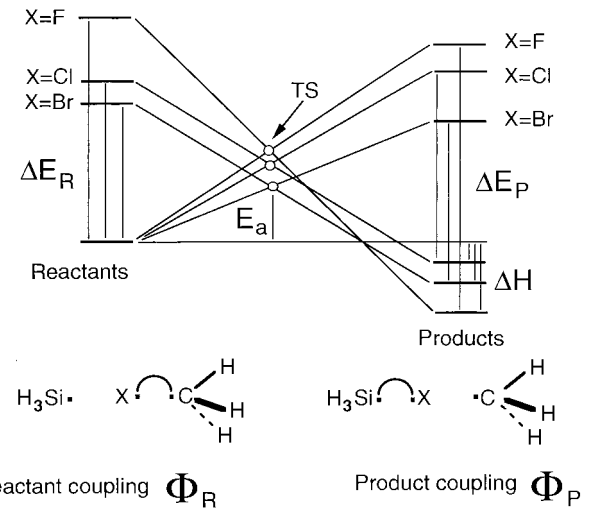

Figure 3. Correlation diagrams for fluorine, chlorine, and bromine abstraction by the $H_3Si\cdot$ radical from FCH_3, $ClCH_3$, and $BrCH_3$.

fluorine and bromine are 17.71 and 1.00 kcal mol^{-1} which are larger and smaller, respectively, than the value of 7.24 kcal mol^{-1} found for chlorine (the barrier for bromine agrees very well with the experimental values reported in the previous section). The diabatic diagram where we compare the fluorine, chlorine, and bromine abstraction is shown in Figure 3. The definition of the reactant and product diabatics is the same as that given in Figure 2. In this case, to roughly evaluate the change of ΔE_R and ΔE_P on passing from F to Cl and Br, we must consider the energies of the C−F, C−Cl, and C−Br bonds in the case of ΔE_R (112.8,[19] 83.5,[16] and 70.0 kcal mol^{-1},[20] respectively) and those of the Si−F, Si−Cl, and Si−Br bonds in the case of ΔE_P (129.0,[21] 110.0,[18] and 82.0[22] kcal mol^{-1}, respectively). The values of ΔH for fluorine, chlorine, and bromine abstraction at the B3LYP/6-31G* level are −34.88, −16.22, and −22.62 kcal mol^{-1}, respectively (see Tables 6 and 8). In the comparison between chlorine and fluorine, it is evident that while the reaction enthalpy favors the fluorine abstraction, the two quantities ΔE_R and ΔE_P, which are larger for fluorine than for chlorine, must favor the chlorine abstraction. ΔE_R and ΔE_P are clearly the dominant factors and determine a larger activation barrier for fluorine than for chlorine. When we compare chlorine with bromine, all three factors concur to

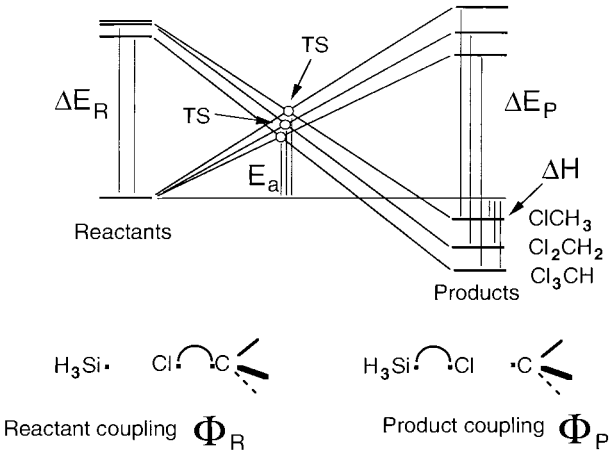

Figure 4. Correlation diagrams for chlorine abstraction by the $H_3Si\cdot$ radical from $ClCH_3$, Cl_2CH_2, and Cl_3CH.

make the activation barrier for bromine abstraction lower than that for chlorine abstraction (the reaction is more exothermic, and both ΔE_R and ΔE_P are smaller for bromine than for chlorine). The overall effect is a very small barrier for bromine abstraction as found at both the experimental and computational levels.

It is worthwhile to outline that in the comparison between F, Cl, and Br the diabatic model is able to predict the correct trend of the activation barriers while the Hammond postulate fails. On the basis of the relative exothermicities of the three abstraction reactions, the Hammond postulate would predict the lowest activation energy in the case of fluorine abstraction. This example points out once again the better performance of the diabatic model, where in determining the position of the transition state and thus the amount of the corresponding activation barrier, we take simultaneously into account not only the reaction enthalpies but also additional factors such as the energies of the breaking and forming bonds. It is evident that only when these two factors have the same trend as the reaction enthalpy or when the reaction enthalpy dominates do the Hammond postulate and the diabatic model give the same information.

An example of this situation, where the two models provide the same answer, can be found in the comparison between $ClCH_3$, Cl_2CH_2, and Cl_3CH for the chlorine abstraction process. The corresponding diabatic diagram is shown in Figure 4. In this case the exothermicity of the reaction increases with the increasing number of the chlorine atoms in the substrate ($\Delta H = -16.22$, -25.01, and -34.35 kcal mol^{-1} for $ClCH_3$, Cl_2CH_2, and Cl_3CH, respectively, as reported in Table 6). ΔE_R should be very similar for $ClCH_3$ and Cl_2CH_2, since the corresponding energies of the C−Cl bond are 83.5[16] and 83.7 kcal mol^{-1},[23] but it should decrease for Cl_3CH, where the C−Cl bond energy becomes 80.9 kcal mol^{-1}.[23] On the other hand, ΔE_P should remain almost identical for the three halomethanes, since it correspond in all three cases to the energy of the Si−Cl bond in $ClSiH_3$. Thus, both ΔH and ΔE_R concur to lower the activation energy along the series $ClCH_3$, Cl_2CH_2, Cl_3CH, as one could expect on the basis of the Hammond postulate. The Hammond postulate also predicts an increasing reactant-like character of the transition state on the basis of the increasing exothermicity of the reaction and agrees with the indication of the diabatic model and with the computational results (θ is greater than 1 and increases along the series $ClCH_3$, Cl_2CH_2, Cl_3CH).

Finally, it is interesting to use a diabatic diagram to compare the reactivity pattern of the silyl radical to that of the methyl radical. The diagram for the reaction between $H_3C\cdot$ and $ClCH_3$ (hydrogen and chlorine abstraction) is reported in Figure 5. The reactant and product configurations can be obtained from those defined in Figure 2 by replacing the pσ orbital on silicon with a pσ orbital on carbon. The value of ΔH for the hydrogen abstraction reaction computed at the B3LYP level is -6.43 kcal mol^{-1} (see note 24), while the corresponding value for the chlorine abstraction is clearly zero. Both ΔE_P and ΔE_R are expected to be larger for the hydrogen abstraction than for the chlorine abstraction; in the former case (ΔE_R), we must compare the energy of the C−H bond (100.9 kcal mol^{-1})[15] with that of the C−Cl bond in $ClCH_3$ (83.5 kcal mol^{-1}),[16] while in the latter (ΔE_P), we must compare the energy of the C−Cl bond (83.5 kcal mol^{-1}) with that of the C−H bond in CH_4 (104 kcal mol^{-1}).[25] Thus, with the methyl radical, both ΔE_R and ΔE_P favor the chlorine abstraction while ΔH has the opposite effect. The effect of ΔH evidently dominates and makes the hydrogen abstraction the easiest process, in agreement with the experimental evidence. The diabatic diagram points out an interesting aspect; the opposite trend of ΔE_R and ΔE_P with respect to ΔH found for $\cdot CH_3$ has the effect of positioning the two crossing points for the hydrogen and chlorine abstraction much closer in energy than in the case of the reaction involving $\cdot SiH_3$. This suggests that with the methyl radical (and generally with alkyl radicals) the difference between the activation barrier for hydrogen abstraction, which is favored, and that for chlorine abstraction must be smaller than in the case of $\cdot SiH_3$. To check this point, we have computed at the B3LYP/6-31G* level the transition state for chlorine abstraction by $\cdot CH_3$ from $ClCH_3$ (see note 26). The activation energy has been found to be 16.76 kcal mol^{-1}, which is 5.97 kcal mol^{-1} higher than that for hydrogen abstraction (10.79 kcal mol^{-1}, from ref 9e), while in the case of $\cdot SiH_3$, the chlorine abstraction is favored by 9.11 kcal mol^{-1}. Furthermore, the relative position of the two crossing points in Figure 5 indicates a reactant-like character of the hydrogen abstraction transition state. Also, this prediction is in agreement with the computed value of the θ parameter, which is greater than 1 for hydrogen abstraction ($\theta = 1.036$ indicating a reactant-like character) and 1 for chlorine abstraction (symmetric transition state).

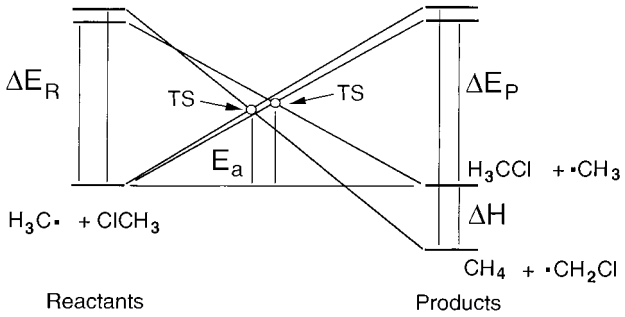

Figure 5. Correlation diagrams for hydrogen and chlorine abstraction by the $H_3C\cdot$ radical from $ClCH_3$.

Conclusion

In this paper, we have reported the results of a theoretical study of the hydrogen and chlorine abstraction reactions by silyl ($H_3Si\cdot$) and trichlorosilyl ($Cl_3Si\cdot$) radical from the three chloromethanes $ClCH_3$, Cl_2CH_2, and Cl_3CH. The study compares the results of traditional ab initio methods (HF, MP2, and MP4) with those obtained with DFT-based methods and with the experiment. For the DFT computations, we have used the hybrid B3LYP and the pure BLYP functionals, which both include nonlocal corrections.

These computations have shown the following. (i) The reaction proceeds in one step through a transition state characterized by a collinear or nearly collinear arrangement of the three atoms involved in the process. (ii) At all computational levels, the energy barrier for hydrogen abstraction is much larger than that for chlorine abstraction; thus, chlorine abstraction is the favored process, in agreement with the experimental results. (iii) The only relevant effect of the inclusion of the dynamic correlation (MP2 and DFT levels) on the geometry of TS_1 (hydrogen abstraction) is that of increasing the product-like character, while for TS_2, (chlorine abstraction) a decrease of the reactant-like character at the MP2 level and an increase at the DFT level are observed. (iv) Only negligible changes in the transition-state geometries and activation energies have been found using the 6-311G** basis set; this indicates that additional polarization functions on hydrogen atoms are not essential to obtain a reliable description of these reactions. (v) Even if the inclusion of dynamic correlation significantly lowers the activation barriers with respect to the HF values, these are still quite overestimated at both the MP2 and MP4 levels; furthermore, the effects of fourth-order corrections in the Moller−Plesset treatment are negligible. (vi) Only the DFT approach can provide reasonable values for the activation barriers; in particular, better performance has been obtained with the hybrid functional B3LYP, which provides activation energies in good agreement with the experiment. These results suggest that DFT-based methods can provide better energetics than traditional correlated methods (such as Moller−Plesset perturbation theory) even if the geometrical results are very similar. The calibration performed here suggests that the B3LYP functional can be used extensively to investigate this class of reactions.

Finally we have demonstrated that many mechanistic details of these reactions, that is, the fact that the chlorine abstraction is highly favored with respect to the hydrogen abstraction, the decrease of the barrier with the increasing number of the chlorine atoms in the substrate, the decrease, for a given substrate, of the rate constants for halogen abstraction along the series X = I > Br > Cl > F, and the different reactivity pattern of the silyl radical when compared to that of the alkyl radicals (hydrogen abstraction favored with respect to halogen abstraction), can be rationalized using a simple diabatic model that can be obtained from the results of reliable quantum mechanical computations on reactants and products and from easily available experimental data such as bond energies. This model detects in the bond energies of the breaking and forming bonds and in the change of the reaction enthalpies ΔH (computed using accurate quantum mechanical total energies) the key factors that must be simultaneously taken into account to explain the trends in reactivity experimentally observed.

References and Notes

(1) Giles, J. R. M.; Roberts, B. P. J. *Chem. Soc., Chem. Commun.* **1981**, 360.

(2) (a) Sakurai, H. In *Free Radicals*; Kochi, J. K., Ed.; Wiley: New York, 1973; Vol. 2, p 741. (b) Lappert, M. F.; Lednor, P. W. *Adv. Organomet. Chem.* **1976**, *14*, 345.

(3) (a) Kerr, J. A.; Smith, J. A.; Trotman-Dickenson, A. F.; Young, J. C.; *J. Chem. Soc. A* **1968**, 510. (b) Cadman, P.; Tilsley, G. M.; Trotman-Dickenson, A. F. *J. Chem. Soc. A* **1969**, 1370. (c) Cadman, P.; Tilsley, G. M.; Trotman-Dickenson, A. F. *J. Chem. Soc., Faraday Trans. 1* **1973**, *69*, 914. (d) Aloni, R.; Horowitz, A.; Rajbenbach, L. A. *Int. J. Chem. Kinet.* **1976**, *8*, 673. (e) Chatgilialoglu, C.; Ingold, K. U.; Scaiano, J. C.; Woynar, H. *J. Am. Chem. Soc.* **1981**, *103*, 3231. (f) Chatgilialoglu, C.; Ingold, K. U.; Scaiano, J. C. *J. Am. Chem. Soc.* **1982**, *104*, 5123. (g) Lusztyk, J.; Maillard, B.; Ingold, K. U. *J. Org. Chem.* **1986**, *51*, 2457. (h) Chatgilialoglu, C.; Griller, D.; Lesage, M. *J. Org. Chem.* **1989**, *54*, 2492. (i) Chatgilialoglu, C. *Chem. Rev.* **1995**, *95*, 1229.

(4) Sakurai, H.; Mochida, K.; Hosomi, A.; Mita, F. *Organomet. Chem.* **1972**, *38*, 275.

(5) Ito, O.; Hoteiya, K.; Watanabe, A.; Matsuda, M. *Bull. Chem. Soc. Jpn.* **1991**, *64*, 962.

(6) Davies, A. G.; Griller, D.; Roberts, B. P. *J. Am. Chem. Soc.* **1972**, *94*, 1782.

(7) Abrahamson, H. B.; Wrighton, M. S. *J. Am. Chem. Soc.* **1977**, *99*, 5510.

(8) Parr, R. G.; Yang, W. *Density-Functional Theory of Atoms and Molecules*; Oxford University Press: New York, 1989.

(9) (a) Hohenberg, P.; Kohn, W. *Phys. Rev. B* **1964**, *136*, 864. (b) Kohn, W.; Sham, L. J. *Phys. Rev. A* **1965**, *140*, 1133. (c) Vosko, S. H.; Wilk, L.; Nusair, M. *Can. J. Phys.* **1980**, *58*, 1200. (d) Becke, A. D. *Phys. Rev.* **1988**, *A38*, 3098. (e) Lee, C.; Yang, W.; Parr, R. G. *Phys. Rev.* **1988**, *B37*, 785. (f) Miehlich, A.; Savin, A.; Stoll, H.; Preuss, H. *Chem. Phys. Lett.* **1989**, *157*, 200. (g) Becke, A. D. *J. Chem. Phys.* **1993**, *98*, 5648.

(10) (a) Fitzgerald, G.; Andzelm, J. *J. Phys. Chem.* **1991**, *95*, 10531. (b) Ziegler, T. *Chem. Rev.* **1991**, *91*, 651. (c) Fan, L.; Ziegler, T. *J. Am. Chem. Soc.* **1992**, *114*, 10890. (d) Bottoni, A. *J. Chem. Soc., Perkin Trans. 2*, **1996,** 2041. (e) Bernardi, F.; Bottoni, A. *J. Phys. Chem.* **1997**, *101*, 1912. (f) Bernardi, F.; Bottoni, A.; Calcinari, M.; Rossi, I.; Robb, M. A. *J. Phys. Chem. A* **1997**, *101*, 6310. (g) Bernardi, F.; Bottoni, A.; Miscione, G. P. *Organometallics* **1998**, *17*, 16.

(11) Frisch, M. J.; Trucks, G. W.; Schlegel, H. B.; Gill, P. M. W.; Johnson, B. G.; Robb, M. A.; Cheeseman, J. R.; Keith, T.; Petersson, G. A.; Montgomery, J. A.; Raghavachari, K.; Al-Laham, M. A.; Zakrzewski, V. G.; Ortiz, J. V.; Foresman, J. B.; Peng, C. Y.; Ayala, P. Y.; Chen, W.; Wong, M. W.; Andres, J. L.; Replogle, E. S.; Gomperts, R.; Martin, R. L.; Fox, D. J.; Binkley, J. S.; Defrees, D. J.; Baker, J.; Stewart, J. P.; Head-Gordon, M.; Gonzalez, C.; Pople, J. A. *Gaussian 94*, revision B.2; Gaussian, Inc.: Pittsburgh, PA, 1995.

(12) (a) Hariharan, P. C.; Pople, J. A. *Theor. Chim. Acta* **1973,** *28,* 213. (b) Krishnan, R.; Binkley, R. S.; Seeger, R.; Pople, J. A. *J. Chem. Phys.* **1980**, *72*, 650. (c) McLean, A. D.; Chandler, G. S. *J. Chem. Phys.* **1980**, *72*, 5639.

(13) Sosa, C.; Schlegel, H. B. *Int. J. Quantum Chem.* **1986**, *29*, 1001; **1987**, *30*, 155.

(14) Pross, A.; Schaik, S. S. *Acc. Chem. Res.* **1983**, *16*, 363. Bernardi, F.; Olivucci, M.; McDouall, J. J. W.; Robb, M. A. *J. Chem. Phys.* **1988,** *89*, 6365

(15) Furuyama, S.; Huybrechts, G. H. *Int. J. Chem. Kinet.* **1969**, *1*, 1.

(16) Benson, S. W. *Thermochemical Kinetics: Methods for the Estimation of Thermochemical Data and Rate Parameters*; John Wiley & Sons: New York, 1968.

(17) Ring, M. A.; Puentes, M. J.; O'Neal, H. E. *J. Am. Chem. Soc.* **1970**, *92*, 4845.

(18) Walsh, R. *Acc. Chem. Res.* **1981**, *14*, 246.

(19) Lias, S. G.; Bartness, J. E.; Liebman, J. F.; Holmes, J. L.; Levin, R. D.; Mallard, W. G. *J. Phys. Chem. Ref. Data* **1998**, *17* (Suppl. 1).

(20) Ferguson, K. C.; Okafo, E. N.; Whittle, E. J. *J. Chem. Soc., Faraday Trans. 1* **1973**, *69*, 295.

(21) Hastie, J. W. *J. Chem. Phys.* **1972**, *57*, 4556.

(22) Gaydon, A. G. *Dissociation Energies and Spectra of Diatomic Molecules*; Chapman and Hall: London, 1968.

(23) Tschuikow-Roux, E.; Paddison, S. *Int. J. Chem. Kinet.* **1987**, *19*, 15.

(24) For the hydrogen abstraction, the value of ΔH has been computed using the total energy values of reactants ($H_3C^{\cdot}$ and $ClCH_3$) and products (CH_4 and $^{\cdot}CH_2Cl$) reported in ref 9e (−539.946 82 and −539.956 71 hartrees, respectively) and the corresponding H_{th} values (47.66 and 47.89 kcal mol^{-1}, respectively).

(25) Gordon, D. M.; Benson, S. W. *Chem. Rev.* **1969**, *69*, 125.

(26) The values of the most relevant geometrical parameters for the chlorine abstraction transition state (B3LYP/6-31G* level) are $a = b =$ 2.119 Å, $\angle ac = 103.1°$. The corresponding total energy and H_{th} values are $E = -539.922\ 52$ hartrees and $H_{th} = 48.00$ kcal mol^{-1}.